Dark matter distribution near the Galactic Center

Alexander F. Zakharov
State Scientific Center – Institute of Theoretical and Experimental Physics,
Moscow, Russia
e-mail:zakharov@itep.ru

Thursday, August 14, 2008, Tuorla, Finland
International Workshop "N-Body:2008"

The talk is based on results of the paper AFZ, F. De Paolis, G. Ingrosso, A.A. Nucita (Salerno University, (PRD, 062001, 2007)

Outline of the talk

- Links and Motivation
- Bright Stars near the Black Hole at the Galactic Center
- Relativistic Celestial Mechanics of the Stars due to an existence of Black Hole and Stellar Cluster
- Hypothesis on Dark Matter Concentration near the Galactic Center
- Limits on Dark Matter Concentrations from Total Gravitating Mass Estimates

- Apocenter Shift Constraints: a Next Step Further
- Progress in Observational Facilities Leads to Strengthen Constraints on DM Concentrations
- Conclusions

Binary BH system

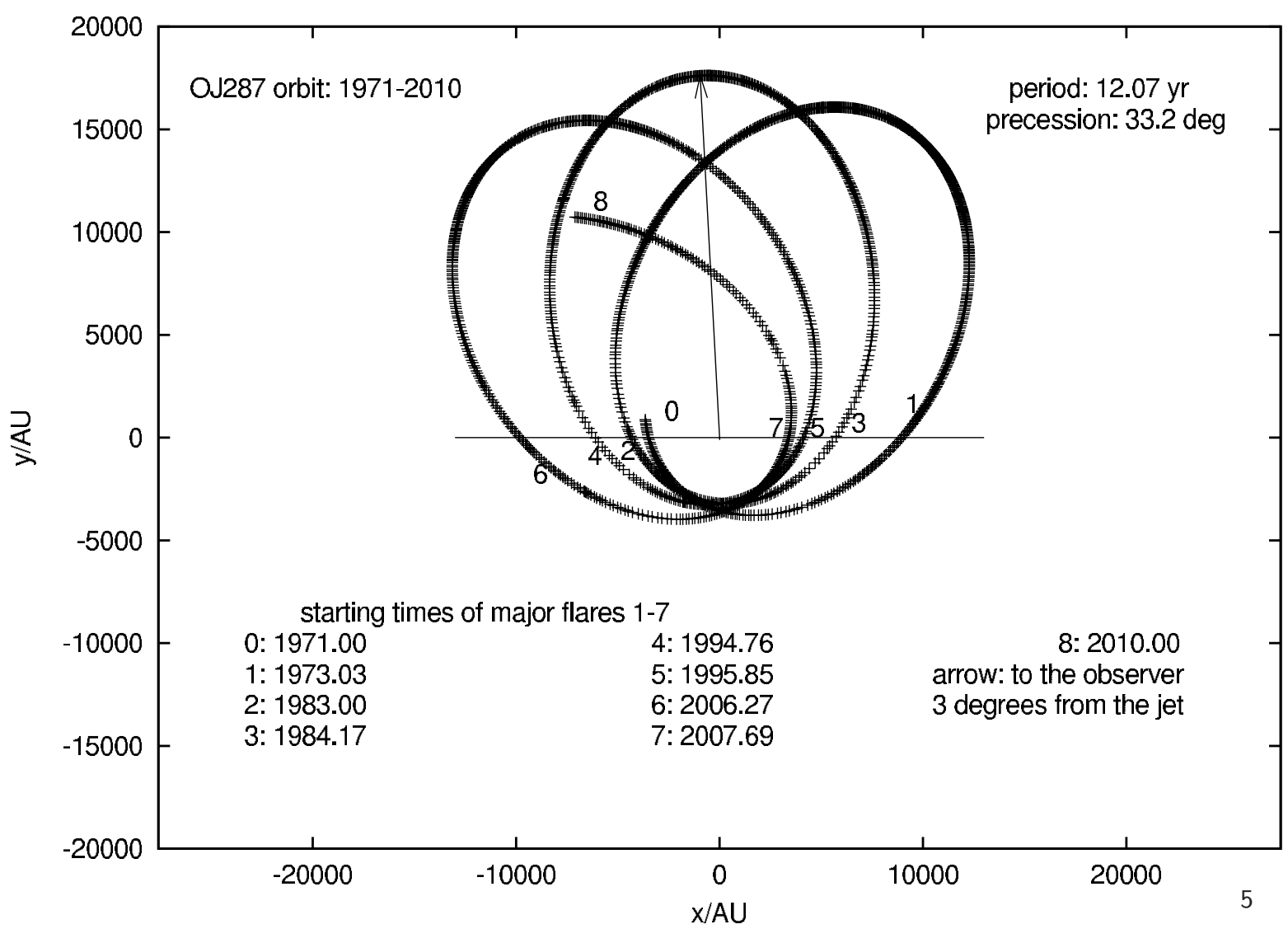

5

FIG. 5.—Orbit of OJ 287 binary system between 1971 and 2010 in the precessing binary model. Giant flares occur subsequent to the disk crossings. Orbital posit of the secondary are shown at the times of giant flares (numbers 1–7). This model assumes that the line of sight (*arrow*) is projected to the orbital plane at angle ϕ, w is 3° from the jet line (normal to the disk). The disk is seen edge-on and is represented by a horizontal line.

Urbain Jean Joseph Le Verrier: Neptune discovery (1846) & Mercury's anomaly (1859) (an invisible ("dark") object or a violation of the Newtonian gravity law)

A connection between our studies and the Le Verrier's discoveries was noted out by Roman Juszkiewicz (2008).

Here I reproduce my understanding these ideas.

In 1846, analyzing trajectories of known objects (planets) and reconstructing potentials and masses and trajectories all objects in the game, Le Verrier predicted an existence of extra (initially unknown (dark)) planet, Neptune and soon afterwards the planet was detected by German

astronomer J.G. Galle. Fritz Zwicky used the same scheme leading to the introduction of dark matter (DM) concept.

Le Verrier discovered Mercury pericenter advance and explained 93% of the observed value, but a supplementary advance 38 arcseconds/century was without an explanation (later on the value was corrected such as 43 arcseconds/century).

Le Verrier's options

- A gravitational field of an invisible matter (planet, asteroids near Sun)
- A deviation from the Newtonian law
- A precision of a model is not good enough

Le Verrier (1876) analyzed information about 25 transits of Vulcan (according to his opinion 19 transits were reliable) and predicted a transit in March 1877 (the planet was not observed). Le Verrier died on 23 September 1877.

Similarly to cosmological DM and DE problems now, different options were considered such as an existence of an extra planet between the Sun

and Mercury (the Vulcan's prediction), a modification mass of Venus by more than 10% and modification of the Newton gravity law (for example, such as Newcomb's modification (1895) of the Newton's law such as $1/r^n$ ($n = 2.0000001574$ for $d\tilde{\omega}/century = 42.34''$, earlier Hall (1894) used $n = 2.00000016$ for $d\tilde{\omega}/century = 43''$).

Exempl. 3. Aſſumentes m & n pro quibuſvis indicibus dignitatum Altitudinis, & b, c pro numeris quibuſvis datis, ponamus vim centripetam eſſe ut $\frac{bA^m + cA^n}{A\,cub.}$, id eſt ut $\frac{b\,in\,\overline{T-X}^m + c\,in\,\overline{T-X}^n}{A\,cub.}$ ſeu (per eandem Methodum noſtram Serierum convergentium) ut $\frac{bT^m - mbXT^{m-1} + \frac{mm-m}{2}bX^2T^{m-2} + cT^n - ncXT^{n-1} + \frac{nn-n}{2}cX^2T^{n-2}\ \&c.}{A\,Cub.}$ & collatis numeratorum terminis, fiet $RGq. - RFq. + TFq.$ ad $bT^m + cT^n$, ut $-Fq.$ ad $-mbT^{m-1} - ncT^{n-1} + \frac{mm-m}{2}XT^{m-2} + \frac{nn-n}{2}XT^{n-2}$ &c. Et ſumendo rationes ultimas quæ prodeunt ubi orbes ad formam circularem accedunt, fit $Gq.$ ad $bT^{m-1} + cT^{n-1}$, ut $Fq.$ ad $mbT^{m-1} + ncT^{n-1}$, & viciſſim $Gq.$ ad $Fq.$ ut $bT^{m-1} + cT^{n-1}$ ad $mbT^{m-1} + ncT^{n-1}$. Quæ proportio, exponendo altitudinem maximam CV ſeu T Arithmetice per unitatem, fit $Gq.$ ad $Fq.$ ut $b + c$ ad $mb + nc$, adeoq; ut 1 ad $\frac{mb+nc}{b+c}$. Unde eſt G ad F, id eſt angulus VCp ad angulum VCP, ut 1 ad $\sqrt{\frac{mb+nc}{b+c}}$. Et propterea cum angulus VCP inter Apſidem ſummam & Apſidem imam in Ellipſi immobili ſit 180 *gr.* erit angulus VCp inter eaſdem Apſides, in Orbe quem corpus vi centripeta quantitati $\frac{bA^m + cA^n}{A\,cub.}$ proportionali deſcribit, æqualis angulo graduum $180\sqrt{\frac{b+c}{mb+nc}}$. Et eodem argumento ſi vis centripeta ſit ut $\frac{bA^m - cA^n}{A\,cub.}$, angulus inter Apſides invenietur $180\sqrt{\frac{b-c}{mb-nc}}$ graduum. Nec ſecus reſolvetur Problema in caſibus

11

I. Newton (Principia) considered a generalization of a gravitational force

$$F = \frac{br^p + cr^m}{r^3}, \tag{1}$$

then

$$d\tilde{\omega} = 2\pi\sqrt{\left|\frac{b-c}{mb-pc}\right|}. \tag{2}$$

Therefore, for $p = 1$ we have

$$F = \frac{br + cr^m}{r^3}, \tag{3}$$

thus if $m \geq 2$, we have generalizations of the Newtonian force with an extra term (Clairaut, 1745; Mikkola 2008, this workshop lecture).

So Clairaut, Hall, Newcomb, Mikkola forces are specific cases of the Newton's relation.

Newcomb's criticism of the Clairaut's law...

For $c = 0$, $F = br^{m-3}$ and

$$d\tilde{\omega} = 2\pi\sqrt{\left|\frac{b}{mb}\right|} = 2\pi\sqrt{\frac{1}{m}}, \tag{4}$$

for $m = 3 - n$ we have

$$d\tilde{\omega} = 2\pi\sqrt{\frac{1}{3-n}} \tag{5}$$

and if $n = 2 + \delta$, then

$$d\tilde{\omega} = 2\pi\sqrt{\frac{1}{1-\delta}} \approx 2\pi(1 + \delta/2) \tag{6}$$

Therefore, following the Le Verrier's way and analyzing carefully trajectories of celestial bodies we can reconstruct gravitational potentials and mass distributions governing motions of celestial bodies.

Figure 3: Urbain Jean Joseph Le Verrier (March 11, 1811 — September 23, 1877).

Introduction

In the last years intensive searches for dark matter (DM), especially its non-baryonic component, both in galactic halos and at galaxy centers have been undertaken (see for example Bertone et al. (2005,2005a) for recent results). It is generally accepted that the most promising candidate for the DM non-baryonic component is neutralino. In this case, the γ-flux from galactic halos (and from our Galactic halo in particular) could be explained by neutralino annihilation (Gurevich et al. 1997,Bergstrom et al. 1998, Tasitsiomi et al. 2002, Stoehr et al. 2003, Prada et al. 2004,Profumo et al. 2005, Mambrini et al. 2005). Since γ-rays are detected not only from high galactic latitude, but also from the Galactic Center, there is a wide spread hypothesis (see, Evans (2004) for a discussion) that a DM concentration might be present at the Galactic Center. In this case the Galactic Center could be a strong source of γ-rays and neutrinos (Bouquet 1989, Stecker

1988, Berezinsky et al. 1994, Bergstrom et al. 1998, Bertone et al. 2004, Gnedin et al. 2004,Bergstrom et al. 2005, Horns 2005, Bertone et al. 2005) due to DM annihilation. Since it is also expected that DM forms spikes at galaxy centers (Gondolo & Silk 1999, Ullio et al. 2001, Merritt et al. 2003) the γ-ray flux from the Galactic Center should increase significantly in that case.

At the same time, progress in monitoring bright stars near the Galactic Center have been reached recently (Genzel et al. 2003,Ghez et al. 2003, Ghez et al. 2005). The astrometric limit for bright stellar sources near the Galactic Center with 10 meter telescopes is today $\delta\theta_{10} \sim 1$ mas and the Next Generation Large Telescope (NGLT) will be able to improve this number at least down to $\delta\theta_{30} \sim 0.5$ mas (Weinberg et al. 2005) or even to $\delta\theta_{30} \sim 0.1$ mas (Weinberg et al. 2005) in the K-band. Therefore, it will be possible to measure the proper motion for about ~ 100 stars with astrometric errors several times smaller than errors in current observations.

The aim of this talk is to constrain the parameters of the DM distribution possible present around the Galactic Center by considering the induced apoastron shift due to the presence of this DM sphere and either available data obtained with the present generation of telescopes (the so called $conservative$ limit) and also expectations from future NGLT observations or with other advanced observational facilities.

Celestial mechanics of S2 like stars for BH+cluster (A.A. Nucita, F. De Paolis, G. Ingrosso, A. Qadir, AFZ, PASP, v. 119, p. 349 (2007))

GR predicts that orbits about a massive central body suffer periastron shifts yielding *rosette* shapes. However, the classical perturbing effects of other objects on inner orbits give an opposite shift. Since the periastron advance depends strongly on the compactness of the central body, the detection of such an effect may give information about the nature of the central body itself. This would apply for stars orbiting close to the GC, where there is a "dark object", the black hole hypothesis being the most natural explanation of the observational data. A cluster of stars in the vicinity of the GC (at a distance < 1 arcsec) has been monitored by ESO and Keck teams for several years.

For a test particle orbiting a Schwarzschild black hole of mass $M_{\rm BH}$, the periastron shift is given by (see e.g. Weinberg, 1972)

$$\Delta\phi_S \simeq \frac{6\pi G M_{BH}}{d(1-e^2)c^2} + \frac{3(18+e^2)\pi G^2 M_{BH}^2}{2d^2(1-e^2)^2c^4} \ , \tag{7}$$

d and e being the semi-major axis and eccentricity of the test particle orbit, respectively. For a rotating black hole with spin parameter $a = |\mathbf{a}| = J/GM_{\rm BH}$, the space-time is described by the Kerr metric and, in the most favorable case of equatorial plane motion (**(a,v)** $= 0$), the shift is given by (Boyer and Price (1965))

$$\Delta\phi_K \simeq \Delta\phi_S + \frac{8a\pi M_{BH}^{1/2} G^{3/2}}{d^{3/2}(1-e^2)^{3/2}c^3} + \frac{3a^2\pi G^2}{d^2(1-e^2)^2c^4} \ , \tag{8}$$

which reduces to eq. (7) for $a \to 0$. In the more general case, **a.v** $\neq 0$, the

expected periastron shift has to be evaluated numerically.

The expected periastron shifts (mas/revolution), $\Delta\phi$ (as seen from the center) and $\Delta\phi_E$ (as seen from Earth at the distance $R_0 \simeq 8$ kpc from the GC), for the Schwarzschild and the extreme Kerr black holes, for the S2 and S16 stars turn out to be $\Delta\phi^{S2} = 6.3329 \times 10^5$ and 6.4410×10^5 and $\Delta\phi_E^{S2} = 0.661$ and 0.672 respectively, and $\Delta\phi^{S16} = 1.6428 \times 10^6$ and 1.6881×10^6 and $\Delta\phi_E^{S16} = 3.307$ and 3.399 respectively. Recall that

$$\Delta\phi_E = \frac{d(1+e)}{R_0}\Delta\phi_{S,K} \ . \tag{9}$$

Notice that the differences between the periastron shifts for the Schwarzschild and the maximally rotating Kerr black hole is at most 0.01 mas for the S2 star and 0.009 mas for the S16 star. In order to make these measurements with the required accuracy, one needs to know the S2 orbit with a precision of at least 10 μas.

The star cluster surrounding the central black hole in the GC could be sizable. At least 17 members have been observed within 15 mpc up to now (Ghez et al. (2005)). However, the cluster mass and density distribution, that is to say its mass and core radius, is still unknown. The presence of this cluster affects the periastron shift of stars orbiting the central black hole. The periastron advance depends strongly on the mass density profile and especially on the central density and typical length scale.

We model the stellar cluster by a Plummer model density profile (Binney & Tremaine (1987))

$$\rho_{CL}(r) = \rho_0 f(r) \ , \qquad \text{with} \qquad f(r) = \left[1 + \left(\frac{r}{r_c}\right)^2\right]^{-\alpha/2} \ , \quad (10)$$

where the cluster central density ρ_0 is given by

$$\rho_0 = \frac{M_{CL}}{\int_0^{R_{CL}} 4\pi r^2 f(r)\ dr}\ , \tag{11}$$

R_{CL} and M_{CL} being the cluster radius and mass, respectively. According to dynamical observations towards the GC, we require that the total mass $M(r) = M_{BH} + M_{CL}(r)$ contained within $r \simeq 5 \times 10^{-3}$ pc is $M \simeq 3.67 \times 10^6\ M_\odot$. Useful information is provided by the cluster mass fraction, $\lambda_{CL} = M_{CL}/M$, and its complement, $\lambda_{BH} = 1 - \lambda_{CL}$. As one can see, the requirement given in eq. (11) implies that $M(r) \to M_{BH}$ for $r \to 0$. The total mass density profile $\rho(r)$ is given by

$$\rho(r) = \lambda_{BH} M \delta^{(3)}(\overrightarrow{r}) + \rho_0 f(r) \tag{12}$$

and the mass contained within r is

$$M(r) = \lambda_{BH} M + \int_0^r 4\pi r'^2 \rho_0 f(r') \, dr' \ . \tag{13}$$

According to GR, the motion of a test particle can be fully described by solving the geodesic equations. Under the assumption that the matter distribution is static and pressureless, the equation of motion of the test particle becomes (see e.g. Weinberg 1972))

$$\frac{d\mathbf{v}}{dt} \simeq -\nabla(\Phi_N + 2\Phi_N^2) + 4\mathbf{v}(\mathbf{v}\cdot\nabla)\Phi_N - v^2\nabla\Phi_N \ . \tag{14}$$

For the S2 star, d and e given in the literature are 919 AU and 0.87 respectively. They yield the orbits of the S2 star for different values of

the black hole mass fraction λ_{BH} shown in Figure 4. The Plummer model parameters are $\alpha = 5$, core radius $r_c \simeq 5.8$ mpc. Note that in the case of $\lambda_{BH} = 1$, the expected (prograde) periastron shift is that given by eq. (7), while the presence of the stellar cluster leads to a retrograde periastron shift. For comparison, the expected periastron shift for the S16 star is given in Figure 15. In the latter case, the binary system orbital parameters were taken from Schödel et al. (2003)) assuming also for the S16 mass a conservative value of $\simeq 10$ $M_\odot$.

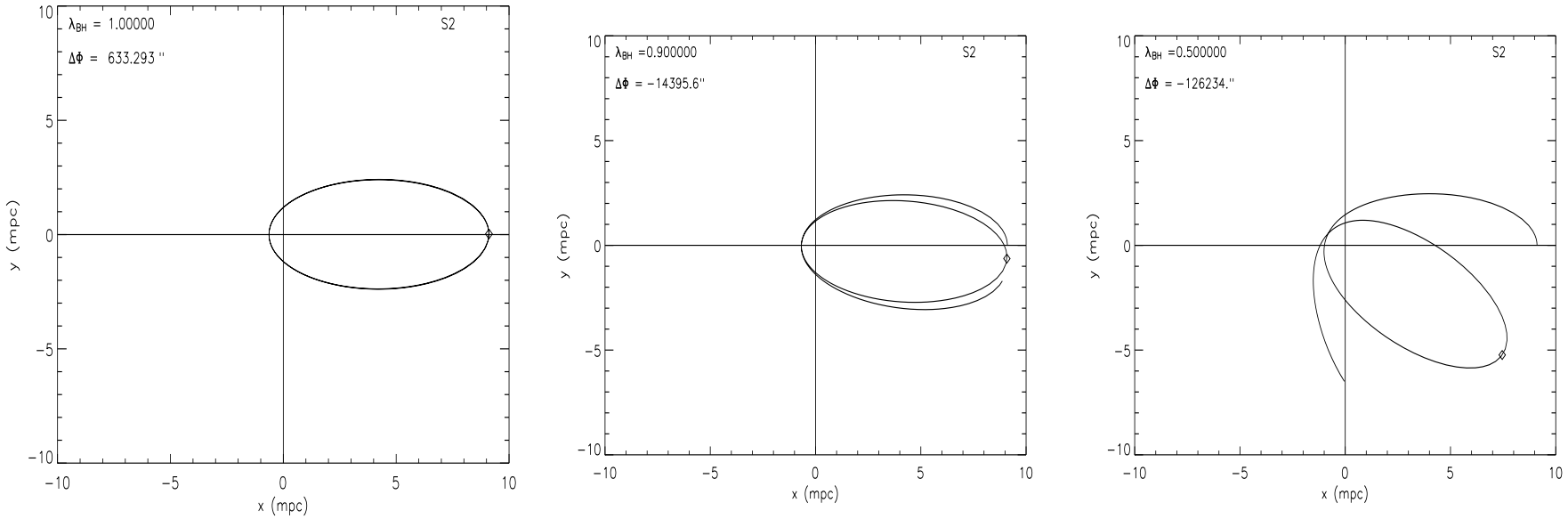

Figure 4: Post Newtonian orbits for different values of the black hole mass fraction λ_{BH} are shown for the S2 star (upper panels). Here, we have assumed that the Galactic central black hole is surrounded by a stellar cluster whose density profile follows a Plummer model with $\alpha = 5$ and a core radius $r_c \simeq 5.8$ mpc. The periastron shift values in each panel is given in arcseconds.

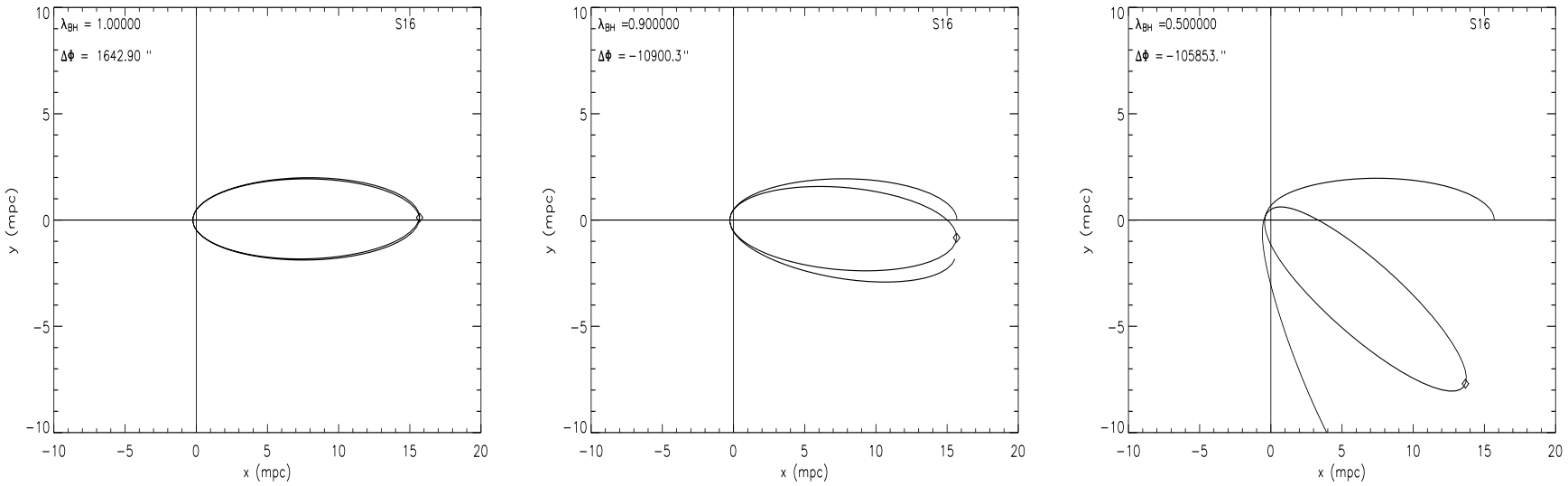

Figure 5: The same as in Figure 4 but for the S16–Sgr A* binary system. In this case, the binary system orbital parameters were taken from Ghez et al. (2005) assuming for the S16 mass a conservative value of $\simeq 10$ $M_{\odot}$.

The mass concentration at the Galactic Center

Recent advancements in infrared astronomy are allowing to test the scale of the mass profile at the center of our galaxy down to tens of AU. With the Keck 10 m telescope, the proper motion of several stars orbiting the Galactic Center black hole have been monitored and almost entire orbits, as for example that of the S2 star, have been measured allowing an unprecedent description of the Galactic Center region. Measurements of the amount of mass $M(< r)$ contained within a distance r from the Galactic Center are continuously improved as more precise data are collected. Recent observations (Ghez et al. (2003)) extend down to the periastron distance ($\simeq 3 \times 10^{-4}$ pc) of the S16 star and they correspond to a value of the enclosed mass within $\simeq 3 \times 10^{-4}$ pc of $\simeq 3.67 \times 10^{6}$ $M_{\odot}$. Several authors have used these observations to model the Galactic Center mass concentration. Here and in the following, we use the three component

model for the central region of our galaxy based on estimates of enclosed mass given by Ghez et al (2003, 2005) recently proposed by Hall and Gondolo (2006). This model is constituted by the central black hole, the central stellar cluster and the DM sphere (made of WIMPs), i.e.

$$M(<r) = M_{BH} + M_*(<r) + M_{DM}(<r) \ , \tag{15}$$

where M_{BH} is the mass of the central black hole Sagittarius A*. For the central stellar cluster, the empirical mass profile is

$$M_*(<r) = \begin{cases} M_* \left(\frac{r}{R_*}\right)^{1.6} \ , & r \leq R_* \\ \\ M_* \left(\frac{r}{R_*}\right)^{1.0} \ , & r > R_* \end{cases} \tag{16}$$

with a total stellar mass $M_* = 0.88 \times 10^6$ M$_\odot$ and a size $R_* = 0.3878$ pc.

As far as the mass profile of the DM concentration is concerned, Hall & Gondolo (2006) have assumed a mass distribution of the form

$$M_{DM}(< r) = \begin{cases} M_{DM}\left(\frac{r}{R_{DM}}\right)^{3-\alpha}, & r \leq R_{DM} \\ M_{DM}, & r > R_{DM} \end{cases} \tag{17}$$

M_{DM} and R_{DM} being the total amount of DM in the form of WIMPs and the radius of the spherical mass distribution, respectively.

Hall and Gondolo (2006) discussed limits on DM mass around the black hole at the Galactic Center. It is clear that present observations of stars around the Galactic Center do not exclude the existence of a DM sphere with mass $\simeq 4 \times 10^6 M_\odot$, well contained within the orbits of the known stars, if its radius R_{DM} is $\lesssim 2 \times 10^{-4}$ pc (the periastron distance of the S16 star in the more recent analysis (Ghez et al. 2005)). However, if one

considers a DM sphere with larger radius, the corresponding upper value for M_{DM} decreases (although it tends again to increase for extremely extended DM configurations with $R_{DM} \gg 10$ pc). In the following, we will assume for definiteness a DM mass $M_{DM} \sim 2 \times 10^5 M_\odot$, that is the upper value for the DM sphere (Hall & Gondolo (2006)) within an acceptable confidence level in the range $10^{-3} - 10^{-2}$ pc for R_{DM}. As it will be clear in the following, we emphasize that even a such small value for the DM mass (that is about only 5% of the standard estimate $3.67 \pm 0.19 \times 10^6\ M_\odot$ for the dark mass at the Galactic Center (Ghez et al. 2005)) may give some observational signatures.

Evaluating the S2 apoastron shift [1] as a function of R_{DM}, one can further constrain the DM sphere radius since even now we can say that there is no evidence for negative apoastron shift for the S2 star orbit at the

[1] We want to note that the periastron and apoastron shifts $\Delta\Phi$ as seen from the orbit center have the same value whereas they have different values as seen from Earth (see Eq. (21)). When we are comparing our results with orbit reconstruction from observations we refer to the apoastron shift as seen from Earth.

level of about 10 mas (Genzel et al. 2003). In addition, since at present the precision of the S2 orbit reconstruction is about 1 mas, we can say that even without future upgrades of the observational facilities and simply monitoring the S2 orbit, it will be possible within about 15 years to get much more severe constraints on R_{DM}.

Moreover, observational facilities will allow in the next future to monitor faint infrared objects at the astrometric precision of about 10 μas (Eisenhauer et al. 2005) and, in this case, previous estimates will be sensibly improved since it is naturally expected to monitor eccentric orbits for faint infrared stars closer to the Galactic Center with respect to the S2 star.

In Fig. 14, the mass profile $M(< r)$ (Ghez et al. 2003) obtained by using observations of stars nearby the Galactic Center is shown (solid line). The dotted line represents the stellar mass profile as given in Eq. (16), while the dashed lines are for DM spheres with mass $M_{DM} \simeq 2 \times 10^5$ M$_\odot$ and

radii $R_{DM} = 10^{-3}$ and 10^{-2} pc, respectively.

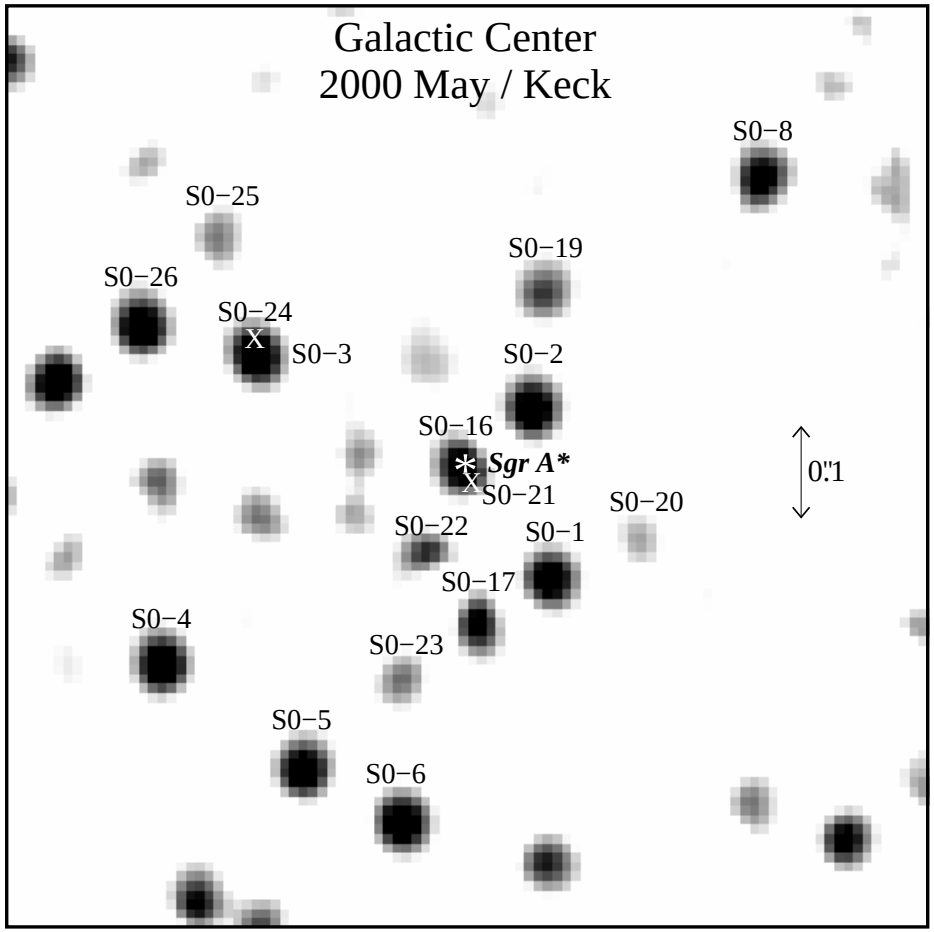

Figure 6: The S2 like star locations near the Black Hole at the Galactic Center (Ghez et al. 2005).

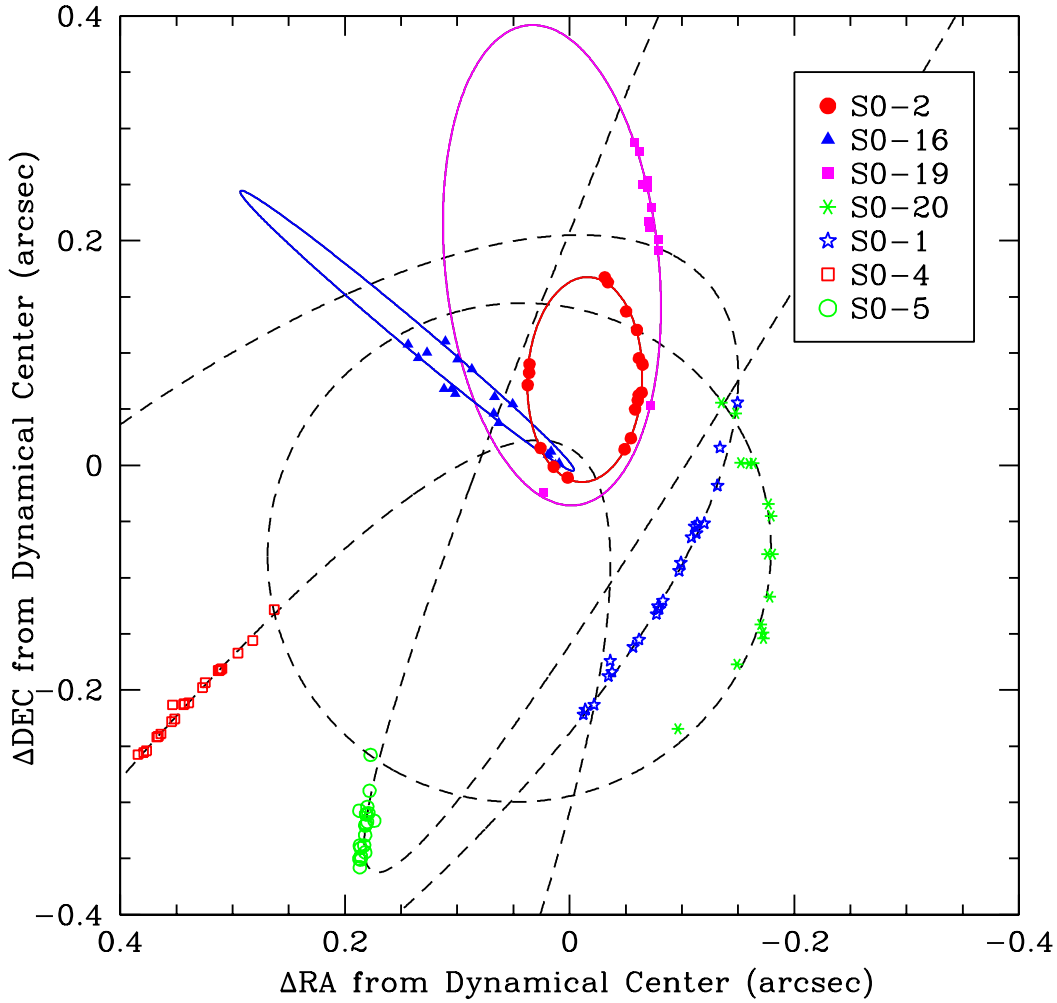

Figure 7: The S2 like star trajectories near the Black Hole at the Galactic Center (Ghez et al (2005)).

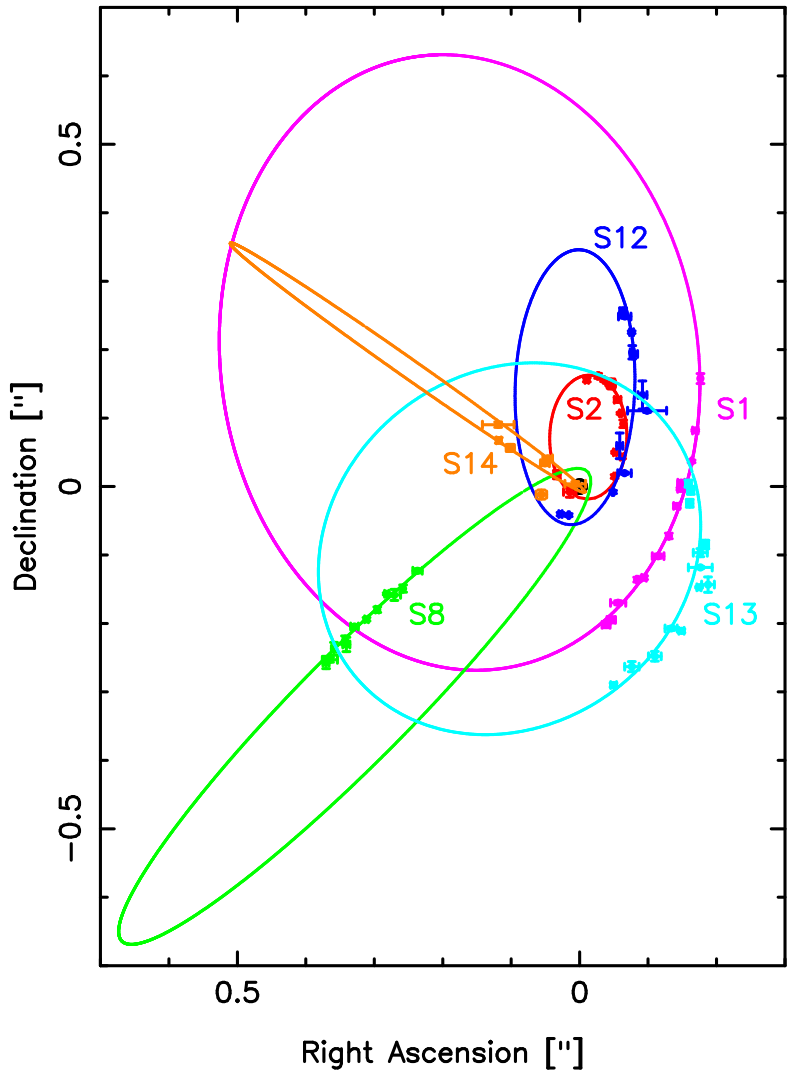

Figure 8: The S2 like star trajectories near the Black Hole at the Galactic Center (Schodel et al (2003)).

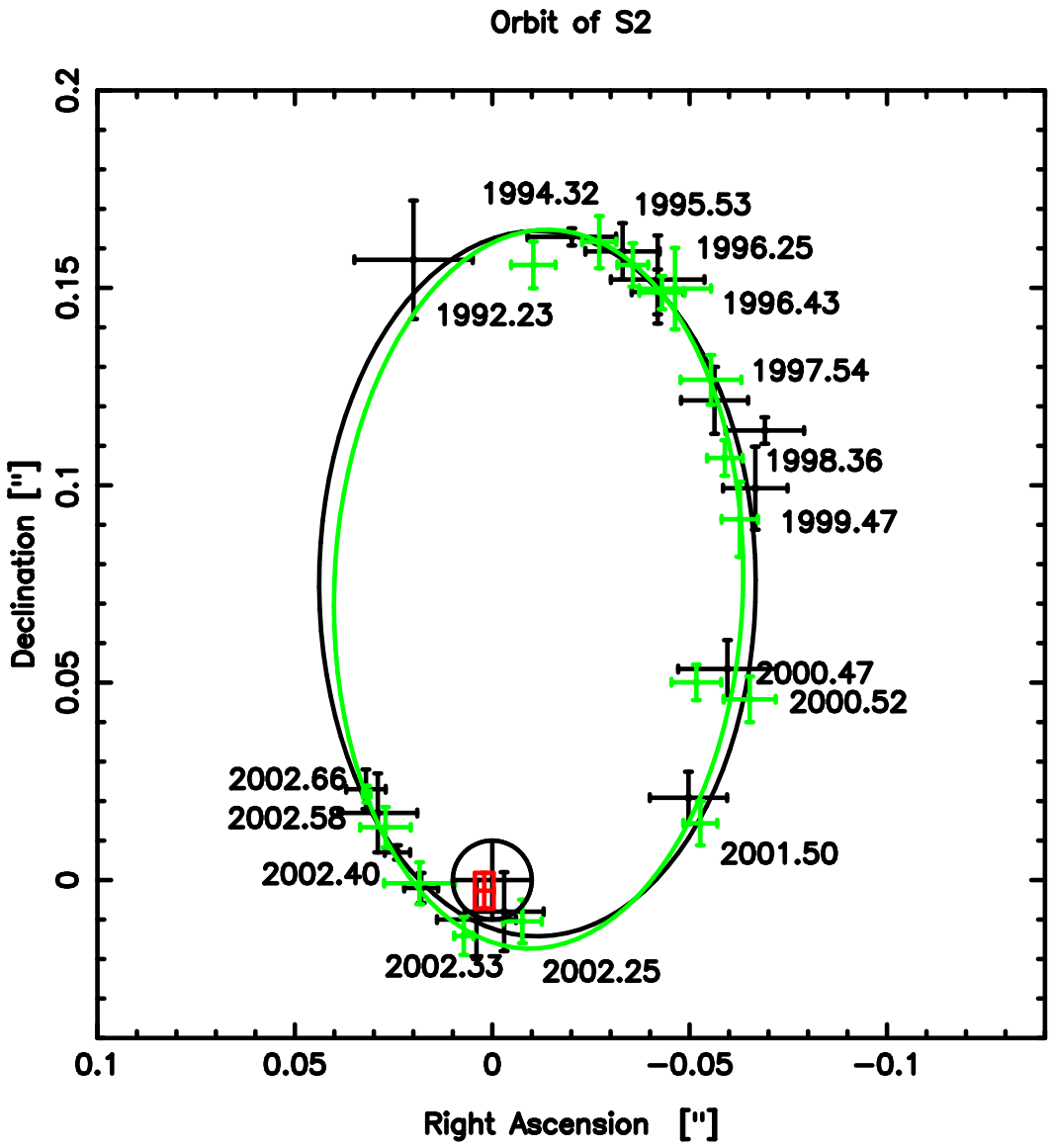

Figure 9: The S2 star trajectory near the Black Hole at the Galactic Center (Schodel et al (2003)).

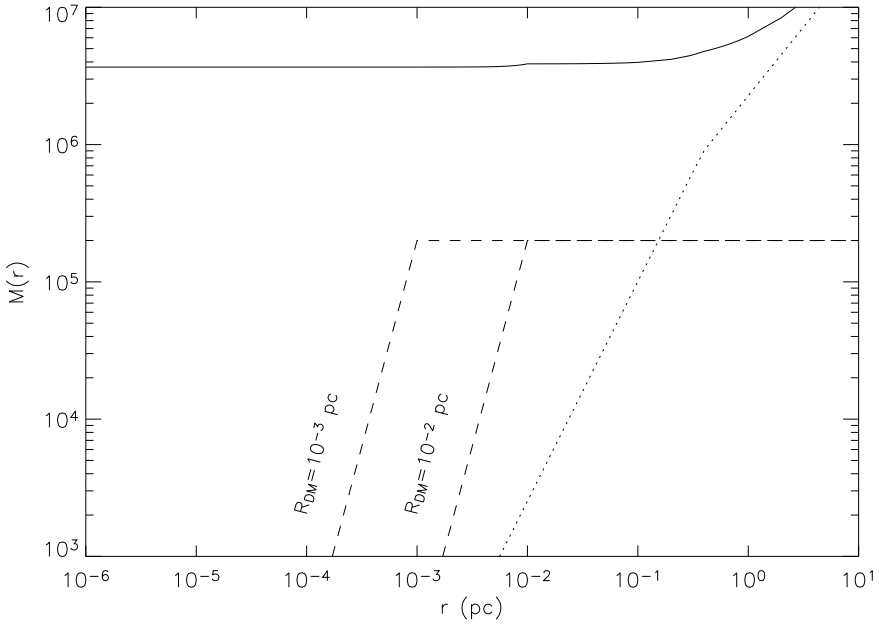

Figure 10: The mass $M(< r)$ obtained in (Ghez et al. 2003) from observations of stars at the Galactic Center is shown (solid line). The dotted line represents the stellar mass profile as given in Eq. (16), while the dashed lines are for DM spheres with radii $R_{DM} = 10^{-3}$ and 10^{-2} pc and mass $M_{DM} \simeq 2 \times 10^5$ $M_\odot$, that corresponds to some acceptable estimate for the upper limit of M_{DM} from Hall and Gondolo (2006).

In the following section, we study the motion of stars as a consequence of the gravitational potential $\Phi(r)$ due the mass profile given in Eq. (15). As usual, the gravitational potential can be evaluated as

$$\Phi(r) = -G \int_r^\infty \frac{M(r')}{r'^2}\, dr' \ . \tag{18}$$

For convenience, in Fig. 11 the gravitational potential due to the total mass (solid line) contained within r is given as function of the galactocentric distance. For comparison, the contributions due to the single mass components, i.e. central black hole, stellar cluster and DM sphere, are also shown.

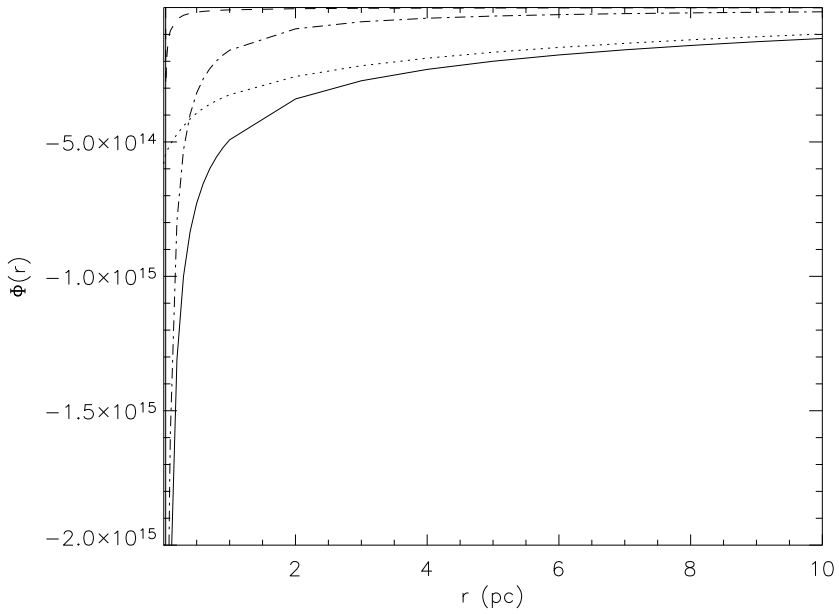

Figure 11: The gravitational potential $\Phi(r)$ (solid line) in cgs units as a function of the galactocentric distance r as due to the mass $M(r)$ in Eq.(15) is shown. For comparison, also the gravitational potentials due to the single mass components, i.e. black hole (dashed line), stellar cluster (dot-dashed line) and DM (dotted line), are also given. Here we assume that DM mass $M_{DM} \simeq 2 \times 10^5$ $M_\odot$ and radius $R_{DM} = 10^{-3}$ pc.

Apoastron Shift Constraints

According to GR, the motion of a test particle can be fully described by solving the geodesic equations. Under the assumption that the matter distribution is static and pressureless, the equations of motion at the first post-Newtonian (PN) approximation become (see e.g. (Fock 1961, Weinberg 1972, Rubilar & Eckart 2001))

$$\frac{d\mathbf{v}}{dt} \simeq -\nabla(\Phi_N + 2\Phi_N^2) + 4\mathbf{v}(\mathbf{v}\cdot\nabla)\Phi_N - v^2\nabla\Phi_N \ . \qquad (19)$$

We note that the PN-approximation is the first relativistic correction from which the apoastron advance phenomenon arises. In the case of the S2 star, the apoastron shift as seen from Earth (from Eq. (21)) due to the presence of a central black hole is about 1 mas, therefore not directly

detectable at present since the available precision in the apoastron shift is about 10 mas (but it will become about 1 mas in 10–15 years even without considering possible technological improvements). It is also evident that higher order relativistic corrections to the S2 apoastron shift are even smaller and therefore may be neglected at present, although they may become important in the future.

As it will be discussed below, the Newtonian effect due to the existence of a sufficiently extended DM sphere around the black hole may cause a apoastron shift in the opposite direction with respect to the relativistic advance due to the black hole. Therefore, we have considered the two effects comparing only the leading terms.

For the DM distribution at the Galactic Center we follow Eq. (17) as done in Hall & Gondolo (2006). Clearly, if in the future faint infrared stars (or spots) closer to the black hole with respect to the S2 star will be monitored (Eisenhauer, (2005)), this simplified model might well not hold

and higher order relativistic corrections may become necessary.

For a spherically symmetric mass distribution (such as that described above) and for a gravitational potential given by Eq. (18), Eq. (19) may be rewritten in the form (see for details Rubilar & Eckart (2001))

$$\frac{d\mathbf{v}}{dt} \simeq -\frac{GM(r)}{r^3}\left[\left(1+\frac{4\Phi_N}{c^2}+\frac{v^2}{c^2}\right)\mathbf{r}-\frac{4\mathbf{v}(\mathbf{v}\cdot\mathbf{r})}{c^2}\right], \qquad (20)$$

r and **v** being the vector radius of the test particle with respect to the center of the stellar cluster and the velocity vector, respectively. Once the initial conditions for the star distance and velocity are given, the rosetta shaped orbit followed by a test particle can be found by numerically solving the set of ordinary differential equations in eq. (20).

In Fig. 4, as an example, assuming that the test particle orbiting the Galactic Center region is the S2 star, we show the Post Newtonian orbits

obtained by the black hole only, the black hole plus the stellar cluster and the contribution of two different DM mass density profiles. In each case the S2 orbit apoastron shift is given. As one can see, for selected parameters for DM and stellar cluster masses and radii the effect of the stellar cluster is almost negligible while the effect of the DM distribution is crucial since it enormously overcome the shift due to the relativistic precession. Moreover, as expected, its contribution is opposite in sign with respect to that of the black hole (Nucita et al. (2007)).

We note that the expected apoastron (or, equivalently, periastron) shifts (mas/revolution), $\Delta\Phi$ (as seen from the center) and the corresponding values $\Delta\phi_E^{\pm}$ as seen from Earth (at the distance $R_0 \simeq 8$ kpc from the GC) are related by

$$\Delta\phi_E^{\pm} = \frac{d(1 \pm e)}{R_0}\Delta\Phi, \tag{21}$$

where with the sign $\pm$ are indicated the shift angles of the apoastron $(+)$

and periastron (-), respectively. The S2 star semi-major axis and eccentricity are $d = 919$ AU and $e = 0.87$ (Ghez et al. 2005).

In Fig. 16, the S2 apoastron shift as a function of the DM distribution size R_{DM} is given for $\alpha = 0$ and $M_{DM} \simeq 2 \times 10^5$ $M_\odot$. Taking into account that the present day precision for the apoastron shift measurements is of about 10 mas, one can say that the S2 apoastron shift cannot be larger than 10 mas. Therefore, any DM configuration that gives a total S2 apoastron shift larger than 10 mas (in the opposite direction due to the DM sphere) is excluded. The same analysis is shown in Figs. 17 and 18 for two different values of the DM mass distribution slope, i.e. $\alpha = 1$ and $\alpha = 2$, respectively. In any case, we have calculated the apoastron shift for the S2 star orbit assuming a total DM mass $M_{DM} \simeq 2 \times 10^5$ $M_\odot$. As one can see by inspecting Figs. 16-18, the upper limit of about 10 mas on the S2 apoastron shift may allow to conclude that DM radii in the range about $10^{-3} - 10^{-2}$ pc are excluded by present observations.

We notice that the results of the present analysis allows to further constrain the results (Hall and Gondolo 2006) who have concluded that if the DM sphere radius is in the range $10^{-3} - 1$ pc, configurations with DM mass up to $M_{DM} = 2 \times 10^5\ M_\odot$ are acceptable. The present analysis shows that DM configurations of the same mass are acceptable only for R_{DM} out the range between $10^{-3} - 10^{-2}$ pc, almost irrespectively of the α value.

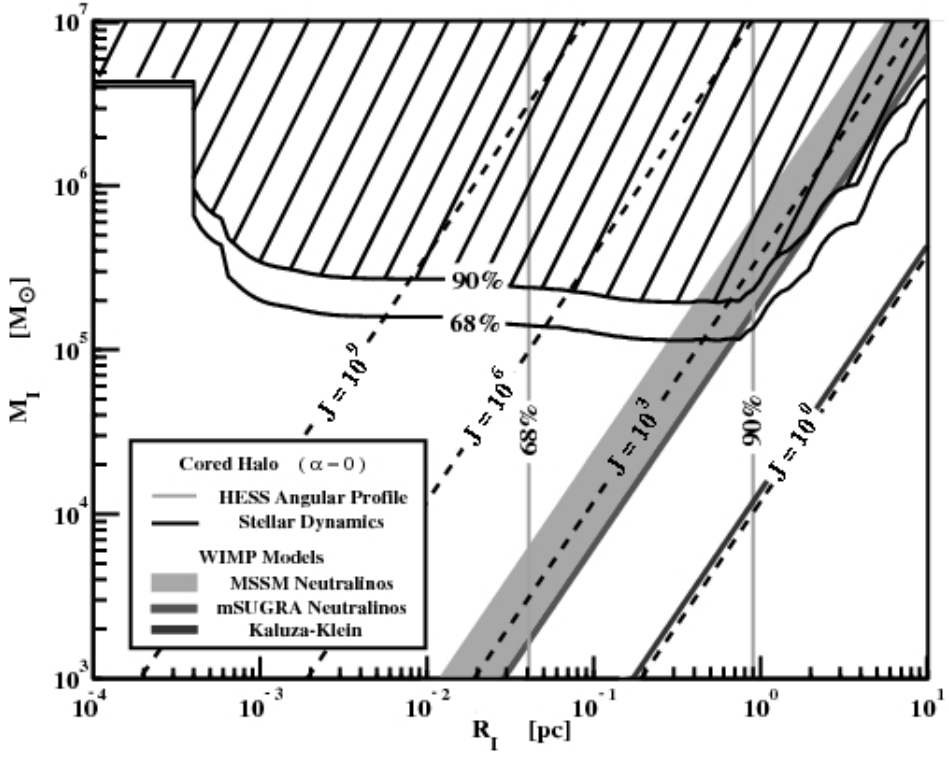

Figure 12: An allowed region for DM distribution from S2 like star trajectories near the Black Hole at the Galactic Center (Hall and Gondolo (2006)).

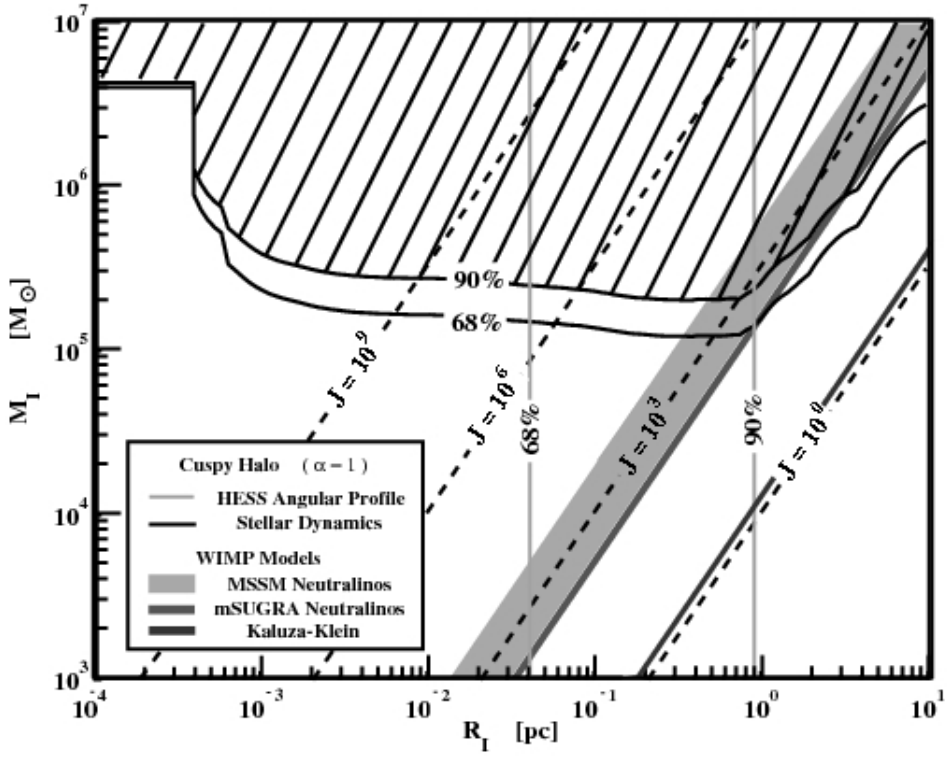

Figure 13: An allowed region for DM distribution from S2 like star trajectories near the Black Hole at the Galactic Center (Hall and Gondolo (2006).

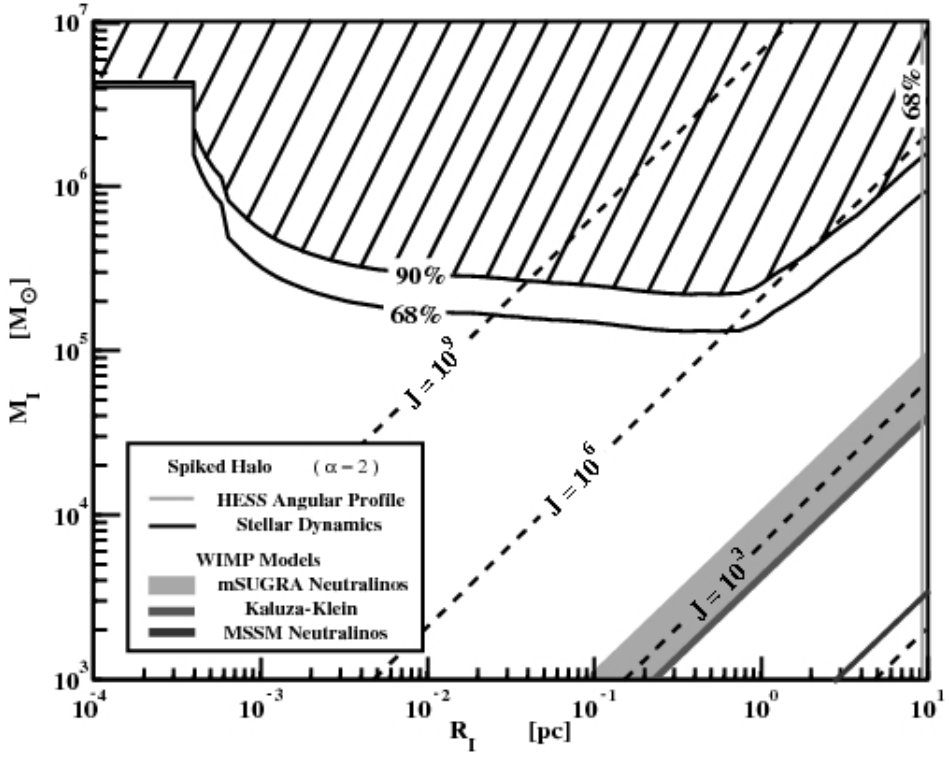

Figure 14: An allowed region for DM distribution from S2 like star trajectories near the Black Hole at the Galactic Center (Hall and Gondolo (2006).

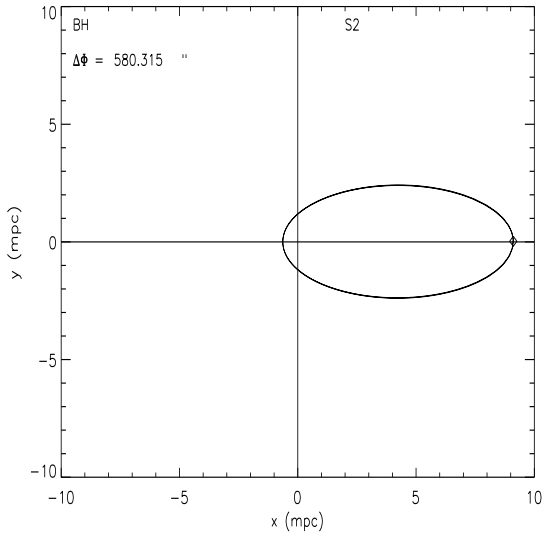
BH
S2
Δϕ = 580.315 ''
y (mpc)
x (mpc)

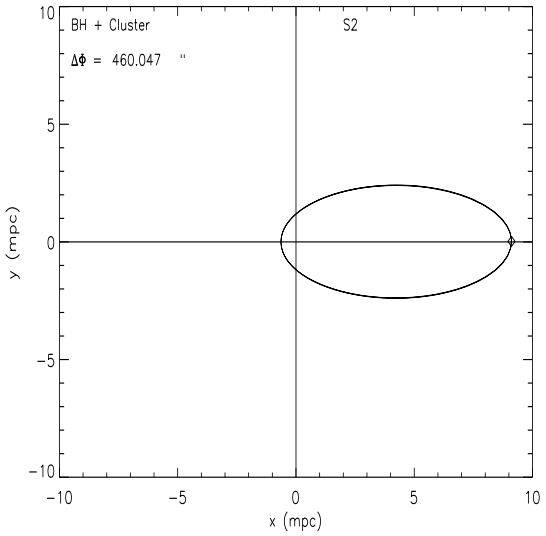
BH + Cluster
S2
Δϕ = 460.047 ''
y (mpc)
x (mpc)

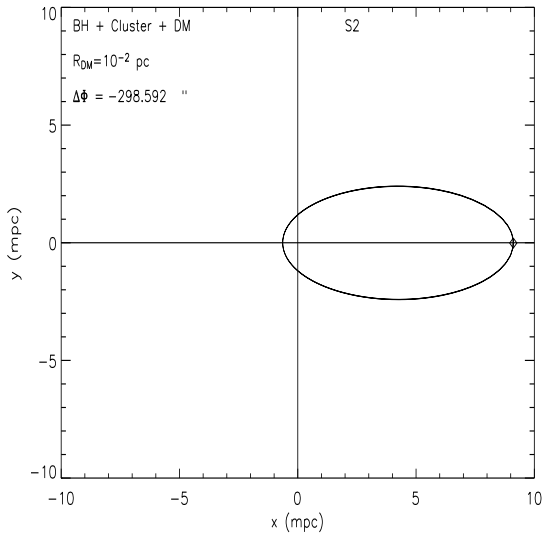
BH + Cluster + DM
S2
R_DM=10^-2 pc
Δϕ = −298.592 ''
y (mpc)
x (mpc)

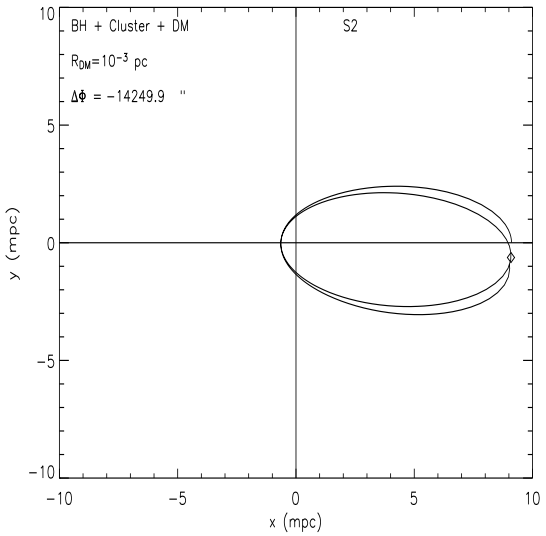
BH + Cluster + DM
S2
R_DM=10^-3 pc
Δϕ = −14249.9 ''
y (mpc)
x (mpc)

Figure 15: PN-orbits for different mass configurations at the Galactic Center. The S2 star has been considered as a test particle and its apoastron shift is indicated in each panel as $\Delta\Phi$ (in arcsec). The top-left panel shows the central black hole contribution to the S2 shift that amounts to about 580 arcsec. The top-right panels shows the combined contribution of the black hole and the stellar cluster (taken following eq. 16) to the S2 apoastron shift. In the two bottom panels the contribution due to two different DM mass-density profiles is added (as derived in eq. 17). We assume that DM mass $M_{DM} \simeq 2 \times 10^5$ $M_\odot$.

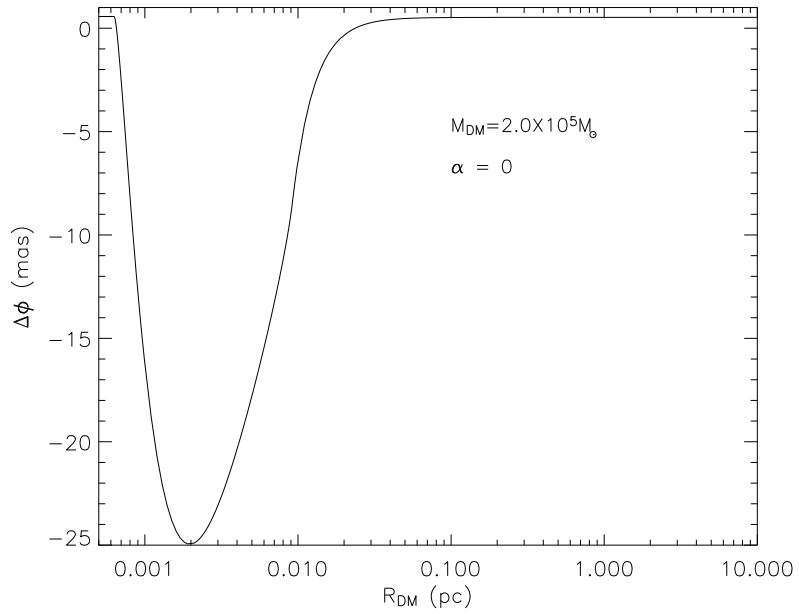

Figure 16: Apoastron shift as a function of the DM radius R_{DM} for $\alpha = 0$ and $M_{DM} \simeq 2 \times 10^5$ $M_\odot$. Taking into account present day precision for the apoastron shift measurements (about 10 mas) one can say that DM radii R_{DM} in the range $8 \times 10^{-4} - 10^{-2}$ pc are not acceptable.

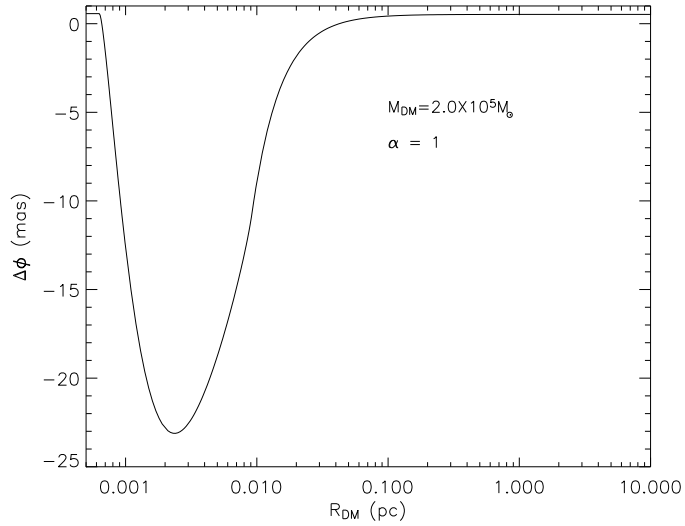

Figure 17: The same as in Fig. 16 for $\alpha = 1$ and $M_{DM} \simeq 2 \times 10^5$ $M_\odot$. As in the previous case one can say that the S2 apoastron shift put severe limits on the DM mass radii that are not acceptable in the range $9 \times 10^{-4} - 10^{-2}$ pc.

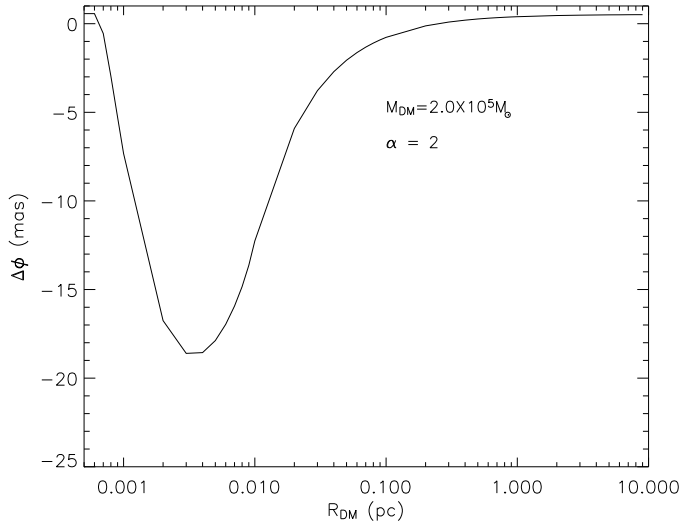

Figure 18: The same as in Fig. 16 for $\alpha = 2$ and $M_{DM} \simeq 2 \times 10^5$ $M_\odot$. As in the previous case one can say that the upper limit to the S2 apoastron shift allows to constrain the DM radius to be out the range $1.0 \times 10^{-3} - 1.1 \times 10^{-2}$ pc.

Discussion

In this paper we have considered the constraints that the upper limit (presently of about 10 mas) of the S2 apoastron shift may put on the DM configurations at the galactic center considered by Hall and Gondolo (2006).

When (in about 10-15 years, even without considering improvements in observational facilities) the precision of S2 apoastron shift will be about 1 mas (that is equal to the present accuracy in the S2 orbit reconstruction) our analysis will allow to further constrain the DM distribution parameters. In particular, the asymmetric shape of the curves in Figs. 16-18 imply that any improvement in the apoastron shift measurements will allow to extend the forbidden region especially for the upper limit for R_{DM}.

In this context, future facilities for astrometric measurements at a level

10 μas of faint infrared stars will be extremely useful (Eisenhauer 2005) and they give a chance to put even more severe constraints on DM distribution.

In addition, it is also expected to detect faint infrared stars or even hot spots (Genzel & Karas 2007) orbiting the Galactic Center. In this case, consideration of higher order relativistic corrections for an adequate analysis of the stellar orbital motion have to be taken into account.

In our considerations we adopted simple analytical expression and reliable values for R_{DM} and M_{DM} parameters following Hall & Gondolo (2006) just to illustrate the relevance of the apoastron shift phenomenon in constraining the DM mass distribution at the Galactic Center. If other models for the DM distributions are considered (see, for instance (Merritt et al. 2007) and references therein) the qualitative aspects of the problem are preserved although, of course, quantitative results on apoastron shifts may be different.

Conclusion

- Present large telescopes and especially forthcoming Next Generation Large Telescope (NGLT) could be treated as a tool for an indirect detection of DM near the Galactic Center

Thank you for your attention